Sensitivity of Numerical Simulations of the Early Rapid Intensification of Hurricane Emily to Cumulus Parameterization Schemes in Different Model Horizontal Resolutions

Xuanli LI and Zhaoxia PU

Department of Atmospheric Sciences, University of Utah, Salt Lake City, Utah, USA

Abstract

A series of numerical experiments are conducted to examine the sensitivity of the numerical simulation of Hurricane Emily's (2005) early rapid intensification to the cumulus parameterization schemes in the advanced research version of Weather Research and Forecasting (WRF) model at different horizontal resolutions. Results indicate that the numerical simulations are very sensitive to the choices of cumulus schemes at 9 km grid spacings. Specifically, with different cumulus schemes, the simulated minimum central sea level pressure (SLP) varies by 41 hPa during the 54 h forecast period. In contrast, only about 10 hPa difference is produced in minimum central SLP by varying planetary boundary layer (PBL) parameterization schemes in the same simulation period. Physical and dynamic mechanisms associated with this sensitivity are investigated. It is found that the intensity of the simulated storm depends highly on the magnitude and structure of surface latent heat flux and convective heating rate over the storm eyewall. The use of cumulus schemes is helpful for the model to reproduce those favorable conditions that cause the storm deepening. However, at 3 km resolution, the cumulus schemes do not result in any notable difference in the storm intensity and track forecasts. Only a slight difference is found in the simulated storm precipitation structure. Compared with cumulus schemes, the PBL schemes have significant impacts on Emily's intensity forecast at 3 km resolution; the minimum central SLP varies by 37 hPa with the use of a different PBL scheme in the WRF model.

1. Introduction

The hurricane forecast could be greatly affected by the deficiency in the numerical modeling system (Rogers et al. 2006). Previous studies showed that the simulations of hurricane intensity and structure were influenced by physical processes in numerical models (Li and Pu 2008; McFarquhar et al. 2006; Braun and Tao 2000), the interactions among the physical processes, as well as the model horizontal grid spacing (Liu et al. 1997; Walsh and Watterson 1997; Karyampudi et al. 1998; Davis and Bosart 2002).

It has long been noticed that surface fluxes in air-sea exchanges are important in the development of tropical cyclones (Byers 1944; Malkus and Riehl 1960). Davis and Emanuel (1988) showed a strong correlation between the rapid deepening of tropical cyclones and warming from the ocean through latent and sensible heat fluxes at ocean surface. Emanuel (1995, 1999) pointed out that the intensification rate of hurricanes depended on the thermodynamic properties of the large scale environment and the air-sea exchange under the core of the storm. Based on their numerical simulations at 4 km grid spacing, Braun and Tao (2000) indicated that the intensity of Hurricane Bob (1991) was more related to the surface fluxes than to the vertical mixing in the planetary boundary layer (PBL). They showed that the ratio of exchange coefficients of enthalpy and momentum was critical to intensity change. Specifically, deeper intensity corresponds to larger exchange ratio, but the deepening rate is not solely decided by the exchange ratio. They attributed this disagreement to storm dynamical response

Corresponding author: Zhaoxia Pu, Department of Atmospheric Sciences, University of Utah, 135 S 1460 E, Rm. 819, Salt Lake City, UT 84112-0110, USA.
E-mail: Zhaoxia.Pu@utah.edu

and complex interactions among the physical processes in the numerical model.

The cumulus parameterization has also been shown to influence the intensity forecast of hurricanes. Challa and Pfeffer (1984) found that the intensification rate and final intensity of tropical cyclones were influenced by the damping effect from cumulus friction in numerical models. Karyampudi et al. (1998) showed that the sensitivity of the intensity forecast to different cumulus parameterizations was mainly due to the difference in the treatment of convective rainfall and latent heat release. Davis and Bosart (2002) claimed that the forecast of intensity and track of tropical cyclone Diana (1984) is sensitive to the model physical parameterization schemes. Specifically, the use of the Kain-Fritsch cumulus scheme has resulted in a well predicted intensification of Diana, partially because of its widespread triggering of convection.

Previous studies indicated that hurricane intensity forecasts were greatly influenced by the representations of the cloud microphysical processes in numerical models. For instance, Zhu and Zhang (2006) presented a pronounced sensitivity of the simulated intensity and inner core structure of Hurricane Bonnie (1998) to various cloud microphysical processes in the MM5 model. They indicated that the weakest storm can be produced by removing all ice particles from the cloud microphysical processes due to greatly reduced latent heat release and much slower autoconversion and accretion processes. They also found that the cooling of melting ice particles and evaporating of cloud and rainwater had a breaking effect on the development of the hurricane. Hence, the most rapid development of the storm was produced when evaporation processes are removed. In recent study, Li and Pu (2008) found that the numerical simulations of the early rapid intensification of Hurricane Emily (2005) are very sensitive to the choice of cloud microphysical scheme in the Weather Research and Forecasting (WRF) model. Specifically, with different cloud microphysical schemes, the simulated minimum central sea level pressure varies by up to 29 hPa.

Although it has been well recognized that all these aforementioned physics processes are important in the mesoscale numerical simulation of hurricanes, there has been a controversy regarding use or not use the cumulus scheme in the high-resolution numerical simulations. Specifically, it is commonly not recommended to use the cumulus schemes in the numerical simulations at horizontal resolutions smaller than 10 km. Thus, many previous studies (e.g., Braun and Tao 2002; Bruan et al. 2006; Liu et al. 1997) have been done without use of cumulus schemes in the high-resolution (e.g., less than 10 km grid spacing) numerical simulations. However, there are also recent studies that have used the cumulus schemes in the numerical simulations at a horizontal resolution of 9 km (Davis and Bosart 2002) and even 6 km (McFarquhar et al. 2006).

Since high-resolution model is usually necessary to the accurate forecast of hurricane intensity forecast, it is important to examine whether these cumulus schemes are really needed in the high-resolution (e.g., the horizontal resolution smaller than 10 km) numerical simulation. In addition, despite the different options regarding the use of cumulus schemes in the numerical simulations, there has not been an explanation as to why the cumulus schemes have a big impact on numerical simulations at one model resolution but not another. The problem is certainly very challenging by nature. In this study, the early rapid intensification of Hurricane Emily (2005) is simulated with various cumulus schemes at different horizontal resolutions. Our goal is to examine the sensitivity of the cumulus scheme on the simulation of rapid hurricane intensification at different horizontal resolutions and also to evaluate how realistic and beneficial it is to use the cumulus scheme at a horizontal resolution of less than 10 km. By choosing an early rapid intensification case, it is also our purpose to investigate the influence of the cumulus scheme to the forecast of hurricane rapid intensification, one of the great challenges in operational hurricane forecasts (Kaplan and DeMaria 2003). Furthermore, considering the interaction between planetary boundary layer (PBL) processes and the cumulus physics in the numerical model and the significantly influence of PBL processes on the simulated hurricane intensity, numerical simulations of the same hurricane are also conducted with the various planetary boundary layer (PBL) parameterization schemes. Simulation results are compared to gain additional insights of the relative sensitivity of both physical processes to the forecast of the rapid intensification of Hurricane Emily.

The paper is organized as follows. Section 2 introduces the hurricane case and numerical model. Sensitivity studies and numerical results examining the sensitivity of various cumulus and PBL schemes

to simulated hurricane intensity at the different resolutions, and the physical processes associated with these sensitivities are analyzed in Section 3 and 4. Concluding remarks are made in Section 5.

2. Description of the Hurricane case and numerical model

2.1 Brief overview of Hurricane Emily (2005)

According to Franklin and Brown (2006), Hurricane Emily (2005) formed on 10 July and dissipated on 21 July 2005. With a maximum surface wind (MSW) speed of 72 m s^{-1} and minimum central sea level pressure (SLP) of 929 hPa, Emily is the strongest and longest-lived hurricane ever on record to form in the month of July. It was also the earliest Category-5 hurricane ever recorded in the Atlantic basin and the only Category-5 hurricane ever recorded before August. It caused $400 million in property damage, 5 direct and 9 indirect fatalities, as well as soil erosion, flooding, and landslides in northeastern Mexico.

In this study, our simulations concentrate on the early rapid intensification period of Hurricane Emily during 1800 UTC 13 July to 0000 UTC 16 July 2005 when the observed minimum central SLP dropped from 1003 to 958 hPa. In the first 36 h of this period, between 1800 UTC 13 and 0600 UTC 15 July, Emily intensified rapidly from a tropical storm to a category-4 hurricane on the Saffir-Simpson hurricane scale, with an extreme deepening rate of about 2 hPa h^{-1}.

2.2 Brief description of the model and experimental design

The Weather Research and Forecasting (WRF) model is a recently developed next-generation mesoscale numerical weather prediction system. The WRF model is based on an Eulerian solver for the fully compressible nonhydrostatic equations, cast in flux conservation form, using a mass (hydrostatic pressure) vertical coordinate. The solver uses a third-order Runge-Kutta time integration scheme coupled with a split-explicit 2nd-order time integration scheme for the acoustic and gravity-wave modes. 5th-order upwind-biased advection operations are used in the fully conservative flux divergence integration; 2nd–6th order schemes are run-time selectable. This study employs an advanced research version of WRF model (ARW) (Skamarock et al. 2005) developed by the National Center for Atmospheric Research (NCAR). The ARW carries multiple physical options for cumulus, microphysical, PBL and radiative physical processes.

In order to test the sensitivity of the numerical simulation of Hurricane Emily's rapid intensification to the cumulus and PBL processes in the WRF model, two sets of simulations are performed. Since it has been well recognized that the cumulus schemes are necessary for a coarse resolution numerical simulation (horizontal resolution greater than 10∼20 km), the experiments in this paper will examine the sensitivities at the fine model grid resolutions, particularly those with less than 10 km grid spacings. The first set of simulations employs a two-way interactive, two-level nested domain with horizontal resolutions of 27 and 9 km. The model is integrated 54 h from 1800 UTC 13 to 0000 UTC 16 July 2005 to examine the sensitivity of numerical simulation of rapid intensification of Emily to three different cumulus and two different PBL parameterization schemes at 9 km horizontal resolution. The second set of simulations adopts a two-way interactive, triple nested domain with horizontal resolutions at 27, 9, and 3 km. Experiments are conducted using two different PBL schemes with and without the cumulus scheme in the 3 km grid spacing. The model vertical structure is comprised of 31 σ levels with the top of the model set at a pressure of 50 hPa. The model domains are given by Fig. 1. The dimensions, grid spaces, and time steps for each domain are listed in Table 1. Initial conditions for the 27-km and 9-km domains and boundary conditions for the 27-km domain are derived from the U. S. National Ceters for Environmental Pre-
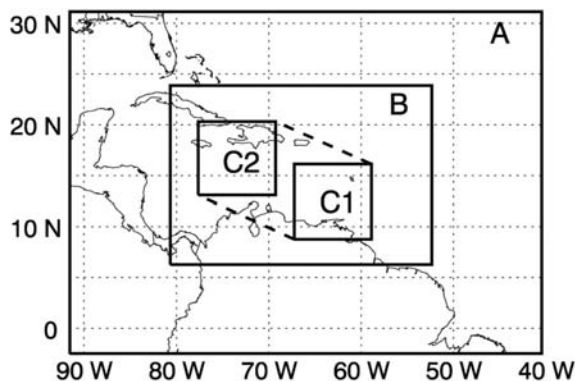
Fig. 1. The locations of the model domains for numerical simulations of Hurricane Emily (2005). Domain A is the 27 km grid and Domains B and C are the nested 9 km grid and 3 km grid. Domain C moved from C1 to C2 at 27 h.

Table 1.   The dimensions, grid spaces, and time steps for model domains

Domain	Dimension ($x \times y \times z$)	Grid Space	Time Step
A	$190 \times 140 \times 31$	27 km	120 s
B	$340 \times 220 \times 31$	9 km	40 s
C	$301 \times 271 \times 31$	3 km	13.3 s

diction's (NCEP) final analysis (FNL) field at $1° \times 1°$ resolution.

In addition to the cumulus and PBL schemes used in the different experiments, Lin microphysics scheme (Lin et al. 1983), a rapid radiative transfer model (RRTM) longwave radiation (Mlawer et al. 1997) and Dudhia shortwave radiation schemes (Dudhia 1989) are employed in all simulations.

3.   Sensitivity at 9 km horizontal resolution

The first set of numerical simulations is conducted to investigate the sensitivity of Emily's forecast to cumulus parameterization schemes at 9 km grid resolution. Three cumulus parameterization schemes, Kain-Fritsch (KF), Betts-Miller-Janjic (BMJ), and Grell-Devenyi (GD) ensemble are compared to demonstrate their sensitivity to numerical simulations of the rapid intensification of Emily. Among these three schemes, the KF scheme is based on a simple cloud model in Kain and Fritsch (1990) and Kain and Fritsch (1993). Along with moist updrafts and downdrafts, it includes the effects of detrainment, entrainment, and simple microphysics. The BMJ scheme (Janjic 1994, 2000), originally derived from Betts-Miller convective adjustment scheme (Betts 1982; Betts and Miller 1986), is commonly used in tropical cyclone simulations (Liu et al. 1997; Braun and Tao 2000; McFarquhar et al. 2006) owing to its good performance over the tropical region. The GD ensemble scheme (Grell and Devenyi 2002) is an ensemble cumulus scheme in which multiple mass-flux type cumulus schemes with different updraft, downdraft, entrain-

ment and detrainment parameters and precipitation efficiencies are run within each grid box and then the results are averaged to give feedback to the model.

The PBL parameterization deals with the vertical sub-grid-scale fluxes due to eddy transports in the whole atmospheric column. Since the interaction between PBL and cumulus processes is usually very important, different PBL parameterization schemes are used along with the cumulus sensitivity experiments. Two PBL schemes, Yonsei University (YSU) PBL scheme and Mellor-Yamada-Janjic (MYJ) scheme are used. The YSU PBL scheme (Hong et al. 2006) is a "nonlocal K" scheme. This scheme employs the counter-gradient fluxes to determine the depth of the PBL, and to constrain the vertical diffusion coefficient to a fixed profile within the PBL. The MYJ scheme is a "local-K" scheme (Janjic 2002). In the scheme, the diffusivity coefficients are parameterized as functions of the local Richardson number. A nonsingular implementation of the Mellor-Yamada Level 2.5 turbulence closure model is used through the full range of atmospheric turbulent regimes. The upper limit of the implementation is decided by total kinetic energy, buoyancy, and shear of the driving flow. In the current ARW model, the surface layer, which calculates surface heat and moisture fluxes, is tied to the particular PBL scheme.

Table 2 summarizes the various sensitivity experiments conducted at 9 km horizontal resolution. All results discussed in this section are from 9 km grid-spacing.

3.1   Intensity

Figure 2 shows the time series of simulated minimum central SLP and maximum surface wind speed (MSW) at 9 km grid-spacing compared with National Hurricane Center (NHC) best track data. Notable differences in storm intensity are found in the experiments with different cumulus and PBL schemes. At the end of the simulations, the

Table 2.   List of coarse resolution (9 km) experiments and their physics options

Simulation	Cumulus scheme	PBL scheme	Other physics
KF+YSU	Kain-Fritsch	Yonsei University	Purdue Lin microphysics scheme
BMJ+YSU	Betts-Miller-Janjic	Yonsei University	
GD+YSU	Grell-Devenyi ensemble	Yonsei University	RRTM longwave radiation
KF+MYJ	Kain-Fritsch	Mellor-Yamada-Janjic	
BMJ+MYJ	Betts-Miller-Janjic	Mellor-Yamada-Janjic	Dudhia shortwave radiation
GD+MYJ	Grell-Devenyi ensemble	Mellor-Yamada-Janjic	
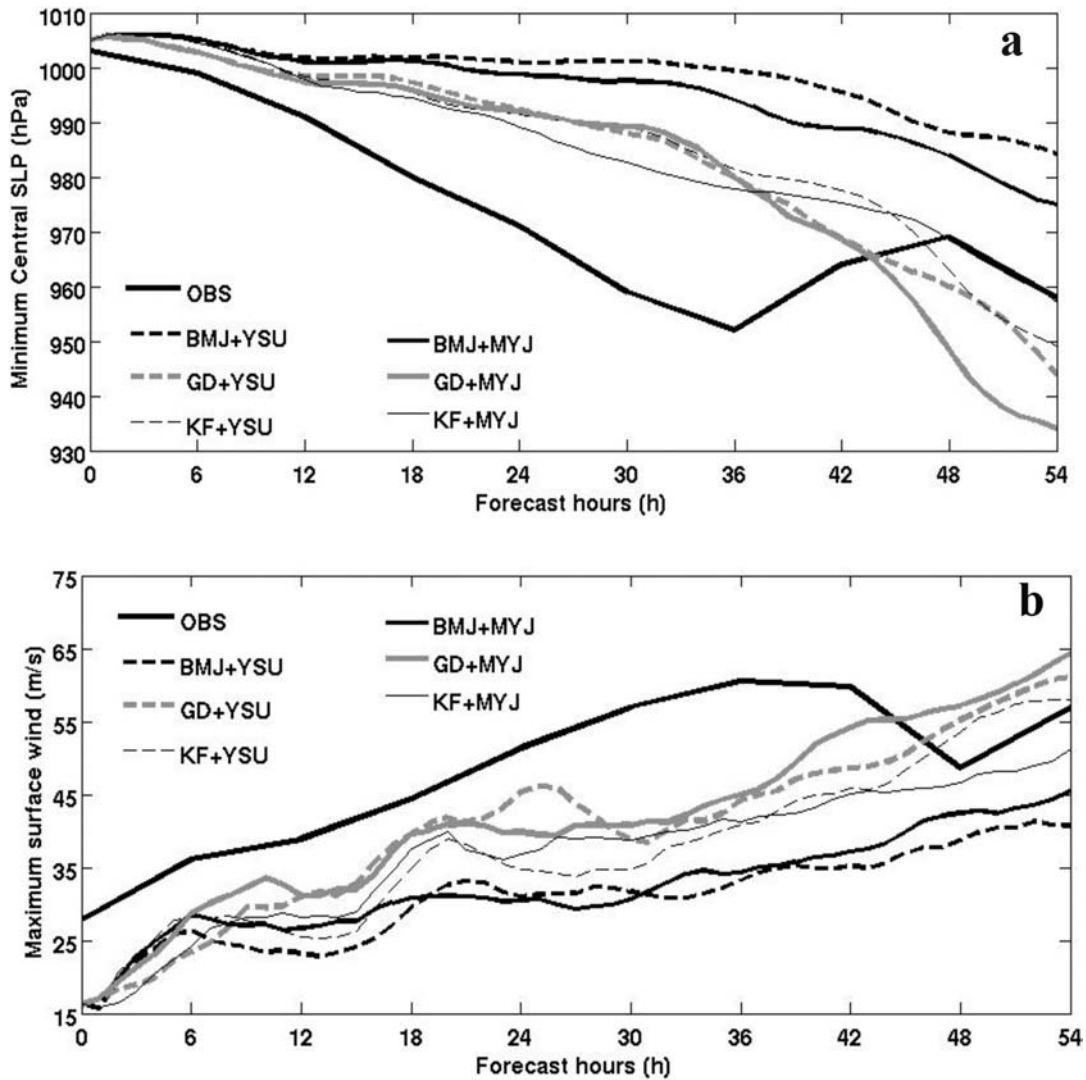
Fig. 2.   Time series of (a) minimum central sea level pressure (hPa) and (b) maximum surface wind speed (m s^{-1}) from the National Hurricane Center best track data and the numerical simulations during 1800 UTC 13 to 0000 UTC 16 July 2005.

strongest storm is produced by experiment GD+MYJ with minimum central SLP of 934 hPa and MSW of 67 m s^{-1}, while the weakest storm produced by experiment BMJ+YSU with the minimum central SLP of 984 hPa and MSW of 40 m s^{-1}.

Significant differences in the forecasted storm intensity are found by varying the cumulus schemes. Specifically, among all cumulus schemes, the BMJ scheme results in the weakest storm and the slowest deepening rate. KF and GD cumulus schemes cause the model to produce similar intensities in the first 33 h. Then, the simulation with the GD cumulus

scheme produces deeper intensity and a faster intensification rate. At the end of the simulations, the forecasted storm with the GD scheme is much stronger than this simulated storm with KF scheme.

The simulated storm intensity is also sensitive to the different in PBL schemes. Although minor differences in intensity forecasts are found by varying PBL schemes in the first 24 h of simulations, the impacts from different PBL schemes increase with time. Compared with the YSU scheme, the MYJ scheme generally causes a deeper intensity forecast in most of the cases. At the end of the simulations,
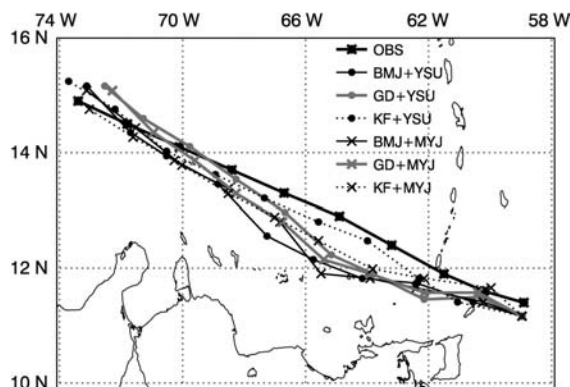
Fig. 3. Forecasts of hurricane track from model simulations during 1800 UTC 13 to 0000 UTC 16 July 2005, compared with the National Hurricane Center best track data. Center locations along the tracks are indicated every 6 h.

a 10 hPa difference in minimum central SLP and 8 m s^{-1} in MSW are found between the experiments with YSU and MYJ scheme regardless of which cumulus schemes are used.

Overall, the intensity forecasts at 9 km grid spacing are sensitive to both cumulus and PBL processes, with larger sensitivity to the cumulus schemes than to the PBL schemes.

3.2 Track

Figure 3 compares the simulated tracks at the 9 km with the NHC best track. In general, similar track forecasts are found when the same cumulus scheme is adopted. This similarity may imply that the track forecast is also more sensitive to the cumulus schemes than to the PBL schemes. Specifically, the KF scheme produces more accurate moving directions compared with the other two cumulus schemes. The best storm track forecast is produced by the experiment that uses KF cumulus and YSU PBL schemes. With the GD cumulus scheme, the model produces southern and western bias in the first 42 h, and northern and eastern bias in the last 12 h of the simulations. The BMJ cumulus scheme causes larger track error than the other two cumulus schemes during most of the simulation period.

3.3 Precipitation

To gain more insight into the influence of different model cumulus and PBL schemes on the structure of Hurricane Emily, Fig. 4 compares the distribution of the 54 h accumulated precipitation

during 1800 UTC 13 to 0000 UTC 16 July 2005 for all experiments. It is apparent that all simulated precipitation show a common pattern, that is, heavier precipitation appears on the southwest of the track in the first 24 h but on the northeast of the track in the last 30 h of the simulations. When the simulated storm is more intense (e.g., in GD+MYJ), a more compact and symmetric precipitation structure is found. The weaker storm (e.g., in BMJ+YSU) exhibits a broader rainfall area with stronger asymmetry.

Since the cumulus scheme represents sub-grid fluxes related to the unresolved convection, it is not surprising that the cumulus scheme has great influence on the simulated rainfall distribution. Specifically, due to the more southerly tracks, larger radii of eyewalls, and the possible influence of topography, the experiments with BMJ cumulus scheme produce much stronger precipitation in the first 24 h of the simulations. In the last 36 h of simulations, much weaker rainfall is produced by the two experiments with the BMJ cumulus scheme, corresponding to the weaker intensities of the two storms. Moreover, the BMJ scheme produces a much more asymmetric structure of precipitation than the other two schemes. In contrast, the GD cumulus scheme results in less precipitation than the BMJ scheme does in the first 18 h due to the further northerly tracks in GD+YSU and GD+MYJ. Meanwhile, larger amounts of precipitation with less asymmetric structures in the last 36 h are generated in experiments with the GD cumulus scheme. These features are especially notable in the experiment GD+MYJ, in which the strongest storm is produced. During the whole simulation period, KF cumulus scheme causes a weaker and narrower precipitation area than the GD cumulus scheme does.

Overall, the results indicate that the simulated rainfall structure of Hurricane Emily has a close relationship with the storm track and intensity. The stronger storms in the experiments with the GD cumulus scheme produce more symmetric precipitation structures. The weaker storms in the experiments with the BMJ cumulus scheme produce less symmetric precipitation structures. Due to possible influence from the topography in South America, more southerly moving storms (e.g., those with the BMJ scheme) produced larger amount of rainfall in the first 24 h of the simulations, while the northerly moving storms (e.g., those with KF cumulus scheme) generate a smaller amount of rainfall.
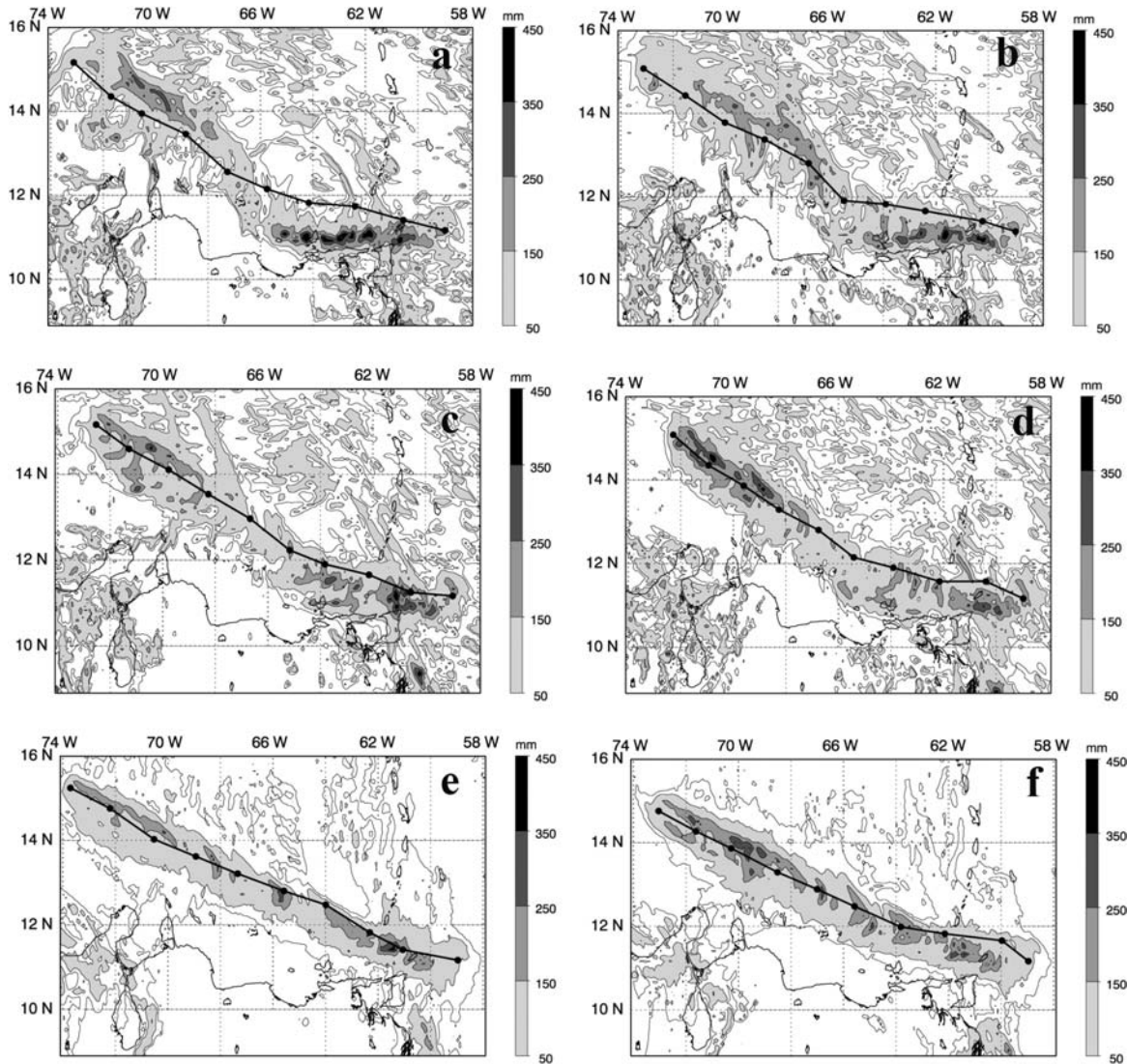
Fig. 4.   54-h accumulated precipitation (mm) from 1800 UTC 13 to 0000 UTC 16 July 2005. a) BMJ+YSU, b) BMJ+MYJ, c) GD+YSU, d) GD+MYJ, e) KF+YSU, f) KF+MYJ.

3.4   Surface latent heat fluxes

In order to examine the physical mechanisms associated with the different cumulus and PBL parameterization schemes that cause the differences in the simulations of Hurricane Emily, several diagnostic variables are investigated.

Figure 5 compares the surface latent heat flux structure at 0000 UTC 16 July 2005 from all experiments. Although it seems the surface latent heat fluxes rely on both cumulus and PBL schemes used in the model, pronounced differences are found in the experiments with various PBL schemes. Com-

pared with the YSU scheme, the use of the MYJ scheme causes the model to produce much stronger surface latent heat fluxes, about 600 w m^{-2} over the maximum value produced by the YSU scheme. This fact corresponds to the deeper storms produced by the experiments with the MYJ scheme. Specifically, the strongest surface energy flux agrees with the strongest hurricane intensity in the experiment GD+MYJ, and the weakest energy supply links to the weakest storm simulated by the experiment BMJ+YSU. However, it should also be noted that the magnitude of the storm deepening rate
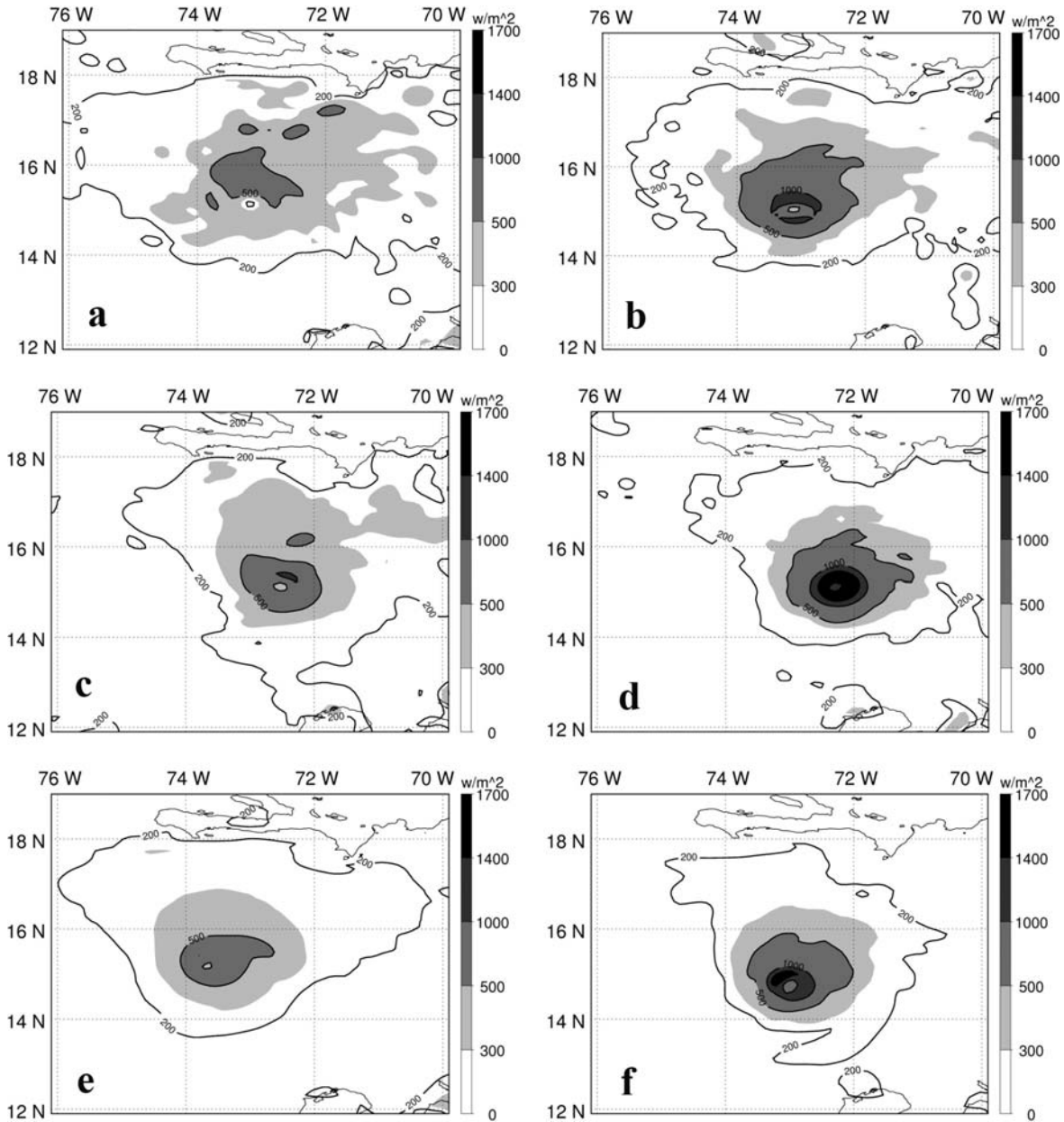
Fig. 5. Surface latent heat flux (w m^{-2}) at 0000 UTC 16 July 2005 from different experiments. a) BMJ+YSU, b) BMJ+MYJ, c) GD+YSU, d) GD+MYJ, e) KF+YSU, f) KF+MYJ.

does not simply depend on the strength of surface energy fluxes. While the experiment BMJ+MYJ produces much stronger surface energy fluxes than the GD+YSU does (about 448 w m^{-2} higher in maximum), the minimum central SLP in BMJ+MYJ is about 32 hPa weaker than that in GD+YSU (Fig. 2).

3.5 Convective heating rate and inner core dynamic structure

Hurricane intensity has a close relationship with the magnitude and structure of the latent heat release (Zhu and Zhang 2006; Li and Pu 2008). Figure 6 compares the distribution of the convective heating rate at 500 hPa from different experiments
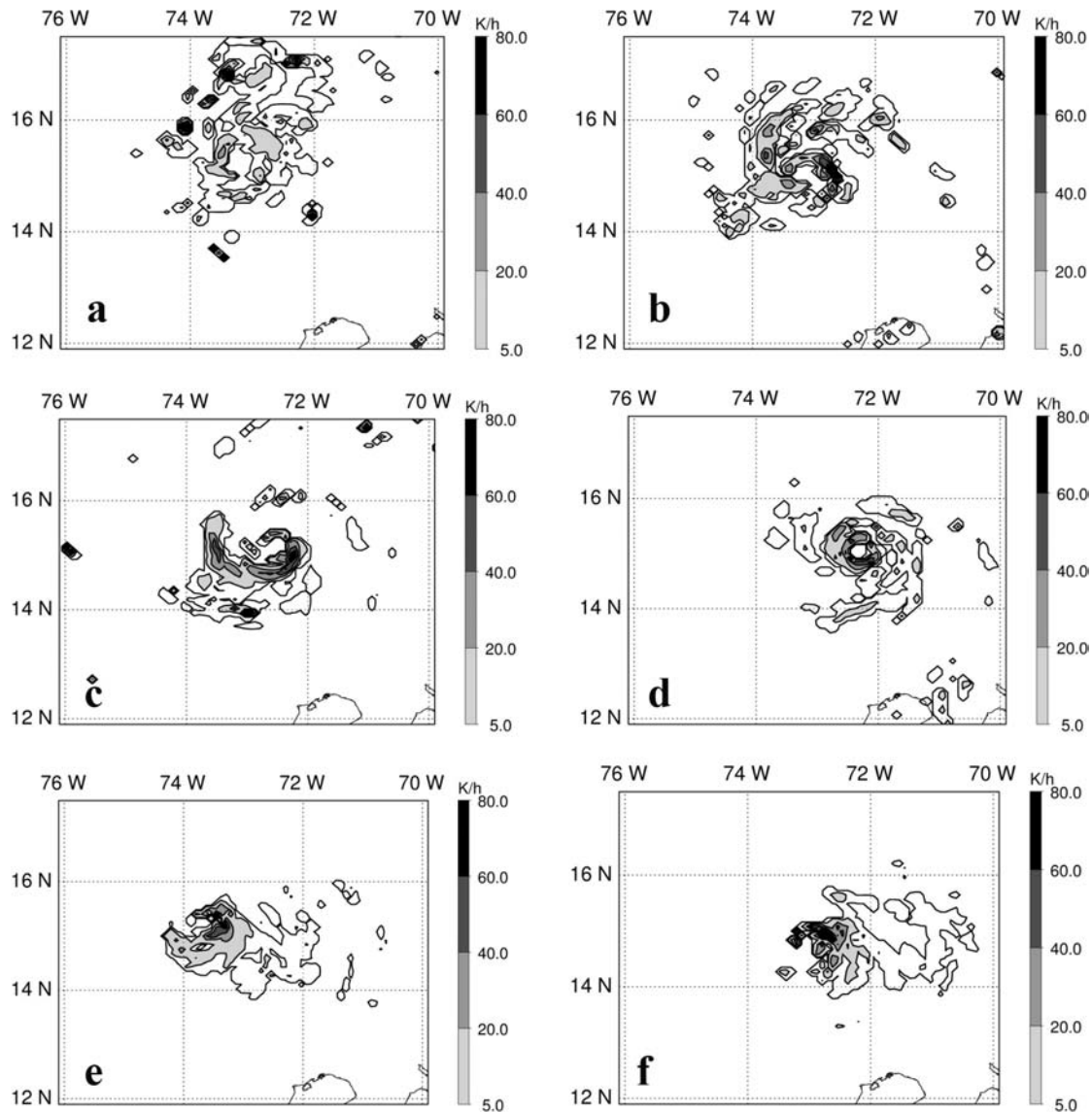
Fig. 6.   Convective heating rate (K h^{-1}) at 500 hPa pressure level on 0000 UTC 16 July 2005 from different experiments. a) BMJ+YSU, b) BMJ+MYJ, c) GD+YSU, d) GD+MYJ, e) KF+YSU, f) KF+MYJ.

at 0000 UTC 16 July 2005. Apparently, the structure of the convective heating rate is largely influenced by the cumulus schemes. Specifically, among all the schemes, the BMJ scheme causes the model to produce weaker and broader convective heating at 500 hPa. Stronger convective heating rates at storm rainband areas and weaker heating at the eyewall regions are also observed. With the GD cumulus scheme, stronger and more symmetric convective heating were produced within the narrow ring of eyewall regions. The KF cumulus scheme

causes stronger asymmetry convective heating structure at the eyewall region with a lower convective heating rate at the storm rainband region. In addition, the use of various PBL schemes influences the distribution of convective heating. In general, experiments with the MYJ scheme produce a stronger convective heating rate over the eyewall region. Compared with the convective heating rate in the different experiments, it is found that the weaker and broader convective heating, as in the experiment BMJ+YSU, corresponds to a slow
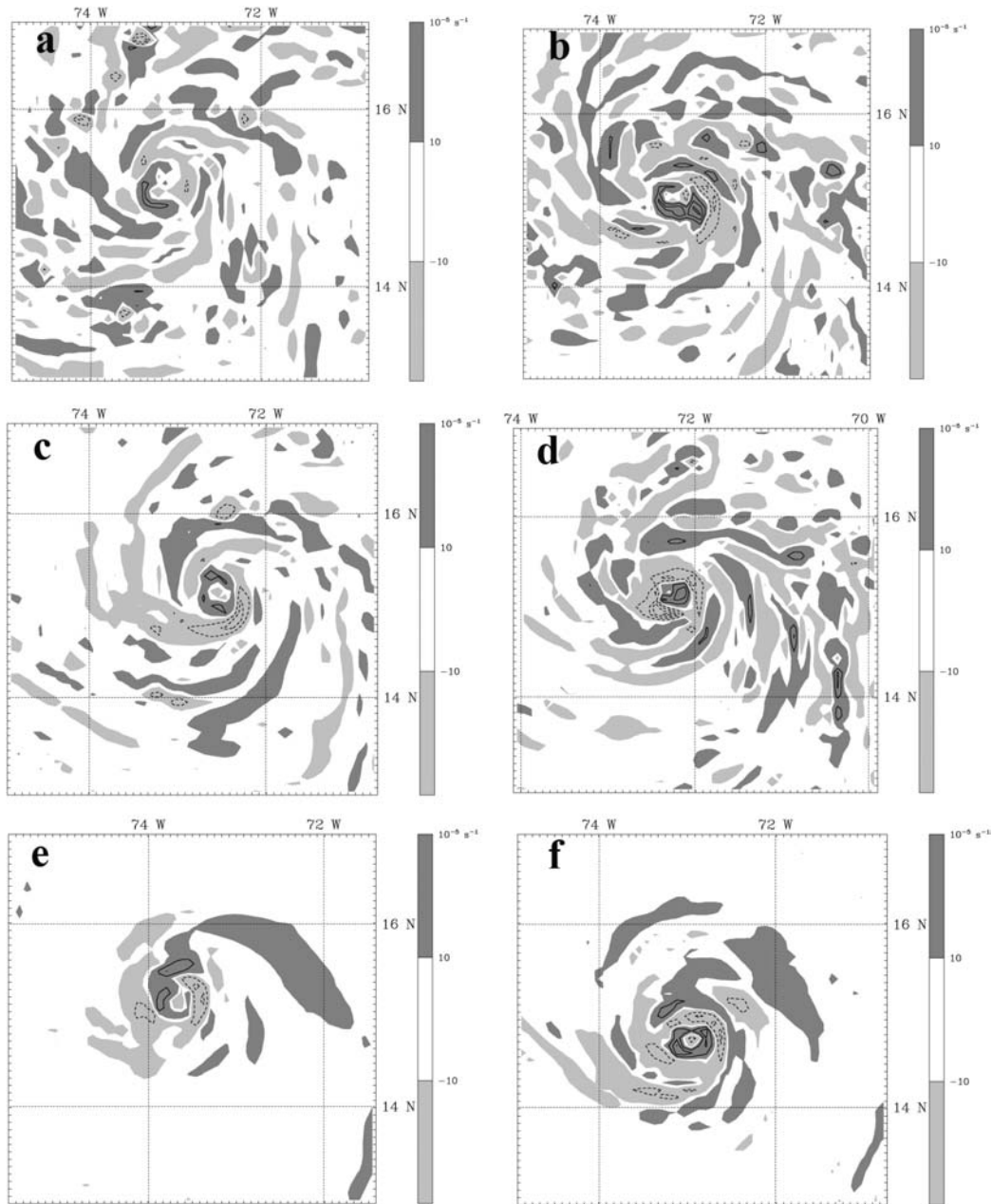
Fig. 7. Divergence (10^{-5} s^{-1}) field at 850 hPa pressure level on 0000 UTC 16 July from different simulations.
a) BMJ+YSU, b) BMJ+MYJ, c) GD+YSU, d) GD+MYJ, e) KF+YSU, f) KF+MYJ.

deepening of the storm. The strong convective heating concentrated at the narrow eyewall region, such as in the experiment GD+MYJ, is responsible for a rapid storm deepening.

As indicated by Willoughby (1988), air flows in a tropical cyclone works in an in-up-and-out pattern. At low levels of the atmosphere, the air flows toward the storm center. This inward air brings heat and moisture from the ocean surface into the storm. At the upper troposphere, outflow exists to compensate the inflow at the low troposphere. This behavior of the air flows is the so-called hurricane secondary circulation. It is a critical factor for maintenance and development of a storm eyewall
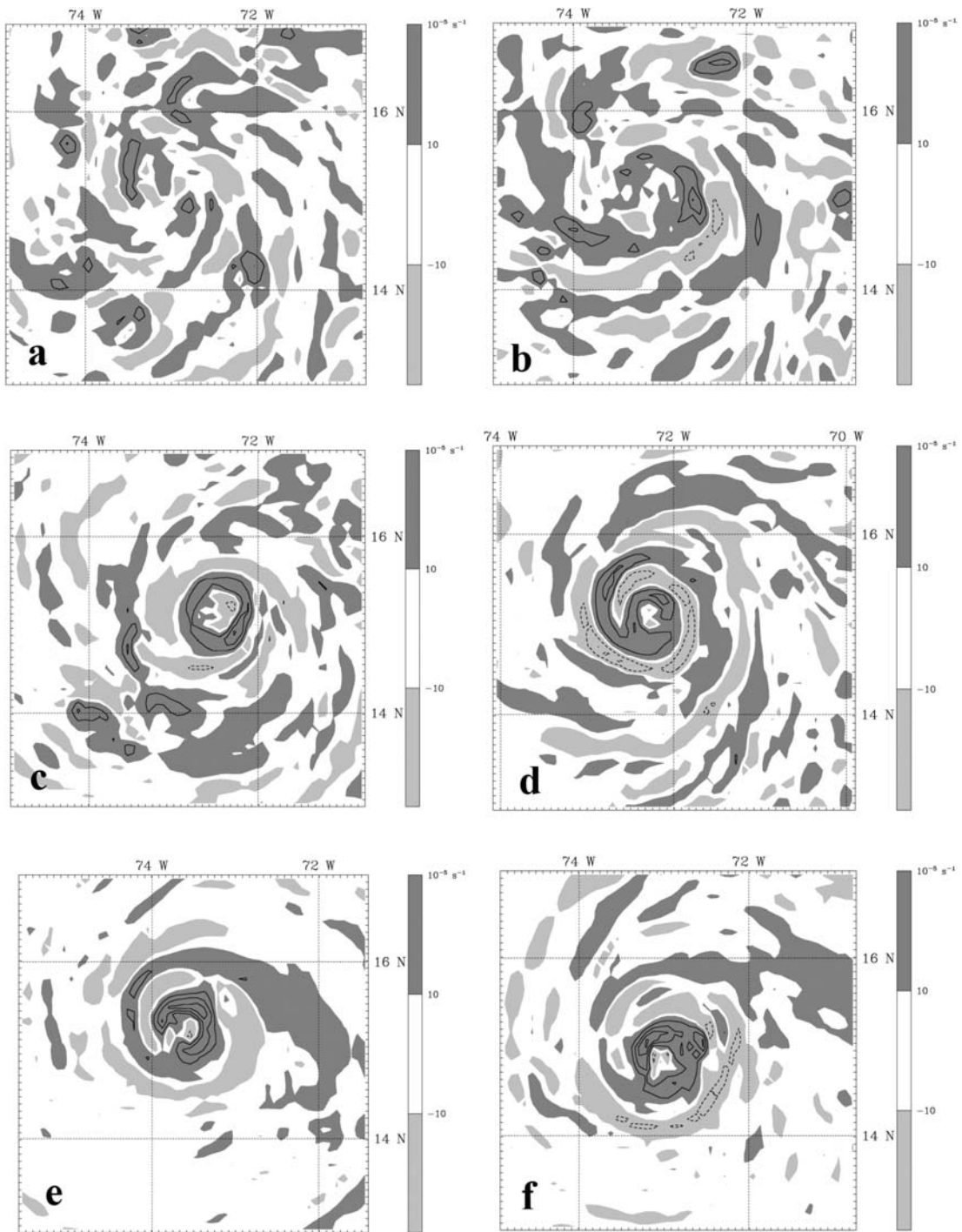
Fig. 8.   Same as Fig. 7, except for 200 hPa pressure level.

(Willoughby 1988). Figures 7, 8 show the divergence field at 850 hPa and 200 hPa at 0000 UTC 16 July. The negative values in the figures represent convergent flows and positive values represent divergent flows. Corresponding to the more intense storm produced by the experiment GD+MYJ, a

Table 3.   List of cumulus sensitivity experiments at different horizontal resolutions and their physics options

Simulation	Cumulus	PBL	Resolution	Other physics
YSU3	N/A	Yonsei University	3 km	Purdue Lin microphysics scheme
YSUCU3	Grell-Devenyi ensemble	Yonsei University	3 km	
MYJ3	N/A	Mellor-Yamada-Janjic	3 km	RRTM longwave radiation
MYJCU3	Grell-Devenyi ensemble	Mellor-Yamada-Janjic	3 km	
YSUNOCU9	N/A	Yonsei University	9 km	Dudhia shortwave radiation
MYJNOCU9	N/A	Mellor-Yamada-Janjic	9 km	

strong, compact convergent inflow at 850 hPa and a strong, well-organized divergent outflow at 200 hPa explain the strong convective heating (Fig. 6) in the narrow ring of eyewall region. Meanwhile, weaker convergent flows at 850 hPa and less compact divergent flows at 200 hPa correspond to weaker storm intensity and convective heating rates in GD+YSU, KF+YSU, and KF+MYJ. Much weaker convergent inflows at 850 hPa and disorganized divergent outflows at 200 hPa are produced by the two experiments with the BMJ schemes. Specifically, the weakest convective heating rate (Fig. 6a) in BMJ+YSU is associated with the weakest convergent inflow at 850 hPa and the weakest divergent outflow at 200 hPa (Figs. 7a, 8a) and also corresponding with the slow intensification rate of the storm in the simulation.

4.   Sensitivity at 3 km horizontal resolution

The results in the previous section generally support the fact that the difference of the cumulus scheme is important in 9 km grid resolution. In this section, simulations are conducted to examine how realistic and beneficial it is to use and not use the cumulus scheme at 9 and 3 km grid spacings.

First of all, experiments YSUNOCU9 and MYJNOCU9 are conducted with the same model set up as in the previous section, except no cumulus scheme is used in the experiments at 9 km grid spacing. In addition, high-resolution simulations are conducted using triple nested domains with horizontal resolutions of 27, 9, 3 km (Fig. 1). Numerical simulations with GD cumulus scheme (YSUCU3 and MYJCU3) and without the cumulus scheme (YSU3 and MYJ3) at 3 km domain are performed and results are compared with those obtained from the simulations at 9 km grid resolution. Same as the experiments in Section 3, two coarse domains with 27 km and 9 km resolutions start at 1800 UTC 13 July 2005. The innermost do-

main at 3 km grid spacing starts at 0600 UTC 14 July 2005 when a more organized storm vortex began to develop. Then the forecast extended till 0000 UTC 16 July 2005 while the domain is moved twice to keep the hurricane nearly at the center of the domain (Fig. 1). For all experiments, RRTM longwave and Dudhia shortwave radiation schemes are adopted. Table 3 lists the physics options for all experiments.

4.1   Intensity and track

Figure 9 compares the time series of the simulated minimum central SLP and MSW from the sensitivity experiments with the NHC best track data. Comparing the intensity forecast from experiment MYJNOCU9 and YSUCOCU9 (Fig. 9) with that from BMJ+MYJ and BMJ+YSU (Fig. 2), it is apparent that the storms could intensify slowly in the experiments without cumulus schemes. Specifically, although the forecasted storm intensity is only about 2 hPa weaker in YSUNOCU compared with that in BMJ+YSU, with MYJ schemes, the forecasted storm intensity from MYJNOCU is about 7 hPa weaker than that with the cumulus scheme (BMJ+MYJ)! The results imply that the cumulus scheme is very important to include for the simulations at 9 km resolution. However, the use of the cumulus scheme in 3 km grid spacing only results in a slight difference in the storm intensity forecasts when compared with the simulations without cumulus schemes (Fig. 9). Specifically, at the end of simulations (54 h), the minimum central SLP (MSW) difference between YSUCU3 and YSU3 is only 1 hPa (5 m s^{-1}) when YSUCU3 produces a slightly deeper storm. Meanwhile, the forecasted storm in MYJCU3 is also only slightly deeper (3 hPa in minimum central SLP and 1 m s^{-1} in MSW) than that in MYJ3. In addition, it should be noted that the intensification rate is greatly influenced by the model PBL scheme. At the end of the
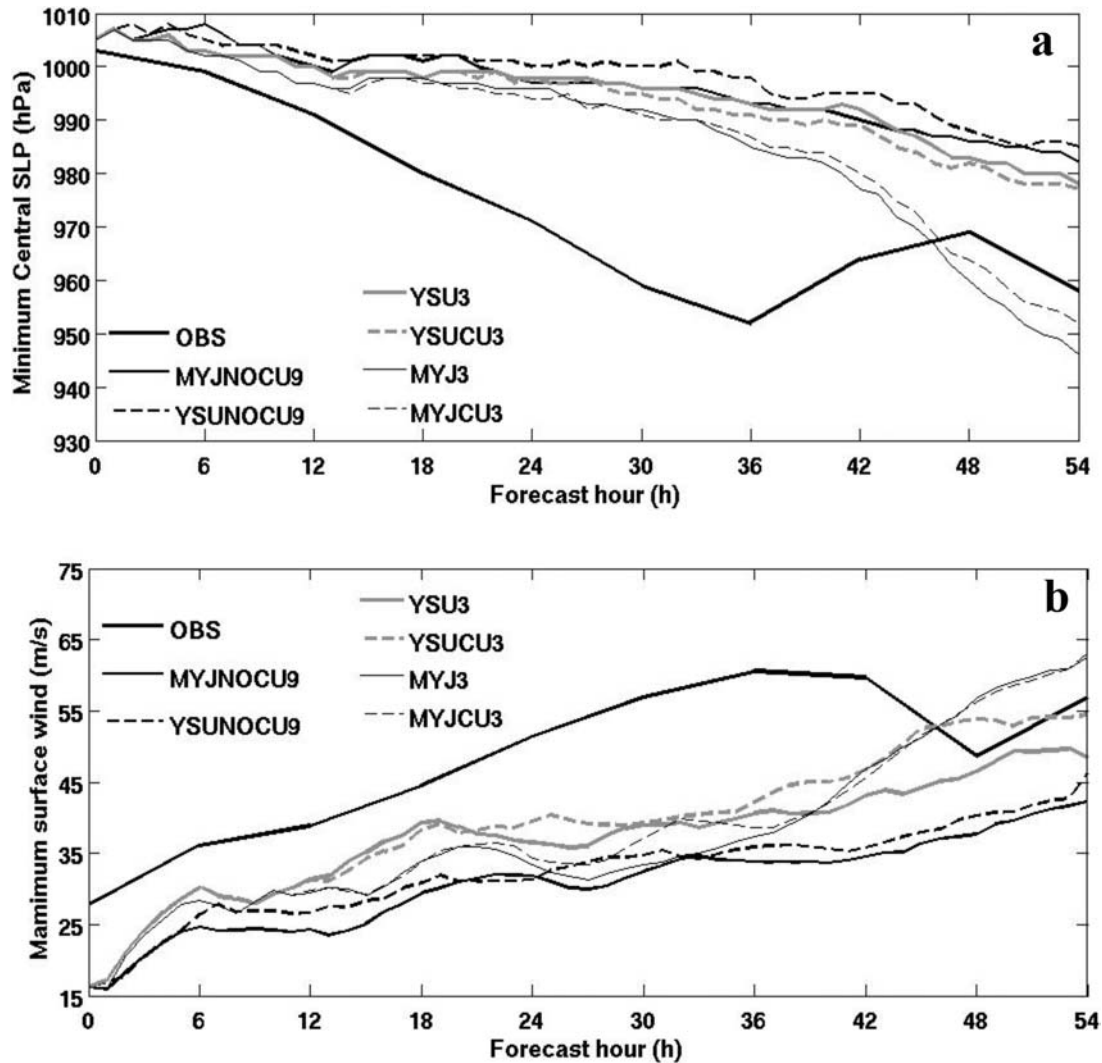
Fig. 9.   Same as Fig. 2, except for the experiments in Section 4.

simulations, up to 37 hPa (14 m s^{-1}) differences in minimum central SLP (MSW) are caused by using two different PBL schemes. Similar to the results in the previous section, the MYJ PBL scheme results in deeper storms.

Figure 10 shows the track forecast from different experiments during 1800 UTC 13 to 0000 UTC 16 July 2005. Without the cumulus scheme, simulations at the 9 km grid spacing experienced large track errors. Including cumulus schemes into the 3 km resolution domain only has a slight influence on the storm track forecast. The maximum track difference is only about 15 km between YSUCU3 and YSU3 and 17 km between MYJCU3 and MYJ3.
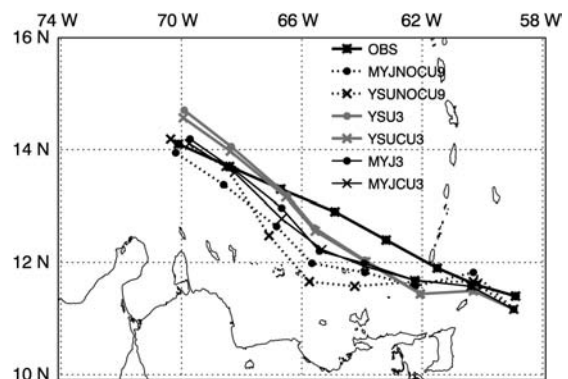
Fig. 10.   Same as Fig. 3, except for the differ-ent experiments in Section 4.

4.2 Precipitation

To further investigate the impact of the cumulus and PBL schemes on the precipitation structure, Fig. 11 compares the hourly rainfall rate from experiments YSU3, YSUCU3, MYJ3, MYJCU3, YSUNOCU9, and MYJNOCU9 at 1800 UTC 15 with the NASA Advanced Microwave Scanning Radiometer for EOS (AMSR-E) satellite rainfall rate observation obtained from the NASA Aqua satellite at 1801 UTC 15 July 2005. Compared with the simulations at 9 km, the simulations at 3 km produce a more realistic small-scale precipitation structure in both eyewall and rainband regions. In addition, for the simulations at 3 km grids, main structures of the rainfall depend largely on the PBL scheme. With the MYJ PBL scheme, the model produced a larger amount of rain with a more symmetric rainfall structure over the storm eyewall. With the YSU scheme, the rain rate is smaller with a strong asymmetric structure. In contrast, the use of cumulus schemes in 3 km grid spacing only has a slight impact on the amount and structure of the precipitation. Only slight differences are found in the rainfall produced by YSU3 and YSUCU3. The forecasted rainfall structures from MYJ3 and MYJCU3 are also very similar. Overall, the simulation with the cumulus scheme at a 3 km resolution (Figs. 11b,d) produces a slightly more realistic rainfall structure although the overall impact from the cumulus scheme is negligible when compare the impact from the PBL schemes.

4.3 Surface latent heat flux

Figure 12 shows the surface latent heat flux distribution from YSU3, YSUCU3, MYJ3, MYJCU3, YSUNOCU9, and MYJNOCU9 at 1800 UTC 15 2005. Compared with the experiments with cumulus schemes (Fig. 5), simulations without the cumulus scheme at the 9 km grid spacing produce smaller surface latent heat flux, which may partially explain the weaker storms produced in the experiments (Fig. 9). Moreover, a significant difference in surface latent heat flux is found between the simulations with different PBL schemes. As shown in Fig. 12, MYJ3 and MYJCU3 produced much stronger surface latent heat flux over the storm eyewall region than YSU3 and YSUCU3 did. The latent heat fluxes in MYJ3 and MYJCU3 show more symmetric features. In contrast, strong asymmetric structures are found in YSU3 and YSUCU3. Compared with its impact at 9 km grid spacing (Figs. 12e,f), the use of the cumulus schemes in the 3 km domains only has a minimum impact on the surface latent heat flux (Figs. 12a–d).

4.4 Vertical velocity

To examine the model dynamic response to the cumulus scheme with different cumulus and PBL schemes, Fig. 13 compares the structures of vertical velocity at 500 hPa generated by different experiments at 1800 UTC 15 July 2005. It seems that the vertical velocities at both 3 km and 9 km grid spacing depend largely on the PBL scheme. Compared with YSU3 and YSUCU3, MYJ3 and MYJCU3 generate much stronger eyewall convection with a more symmetric distribution, corresponding to the stronger storm intensification in the MYJ3 and MYJCU3. In experiments YSUNOCU9 and MYJ-NOCU9, updrafts and downdrafts are very weak in the storm inner core.

The above results indicated that the use of cumulus schemes is very important for the simulations at the 9 km grid spacing. Without the cumulus schemes, the model produces weak vertical velocity and less surface latent heat flux, hence the weak storm intensity. At 3 km grid spacing, the contribution from cumulus schemes to the storm precipitation, surface latent heat flux, and vertical velocity structure is minimal. But, the simulations are extremely sensitive to the variation of the PBL schemes.

5. Concluding remarks

A series of numerical simulations is conducted with the ARW model to examine the impact of cumulus and PBL schemes on the numerical simulations of Hurricane Emily (2005)'s early rapid intensification. Results show the following:

1) At the 9 km horizontal resolution, the storm intensity and deepening rate show a larger sensitivity to the cumulus parameterization than to the PBL scheme. Up to 41 hPa difference in minimum central SLP is generated by using different cumulus schemes, while varying the PBL scheme only results in an 10 hPa difference in minimum central SLP.

2) For simulations at the 9 km grid spacings, the intensities of the simulated storms highly depend on the magnitude and structure of the convective heating rate over the eyewall region. The compact and strong convective heating rate over the eyewall region results in the rapid deepening of the simulated storm in GD+MYJ, while at the same time the broader and weaker convective heating causes the weak intensity simulated in BMJ+YSU. The differ-
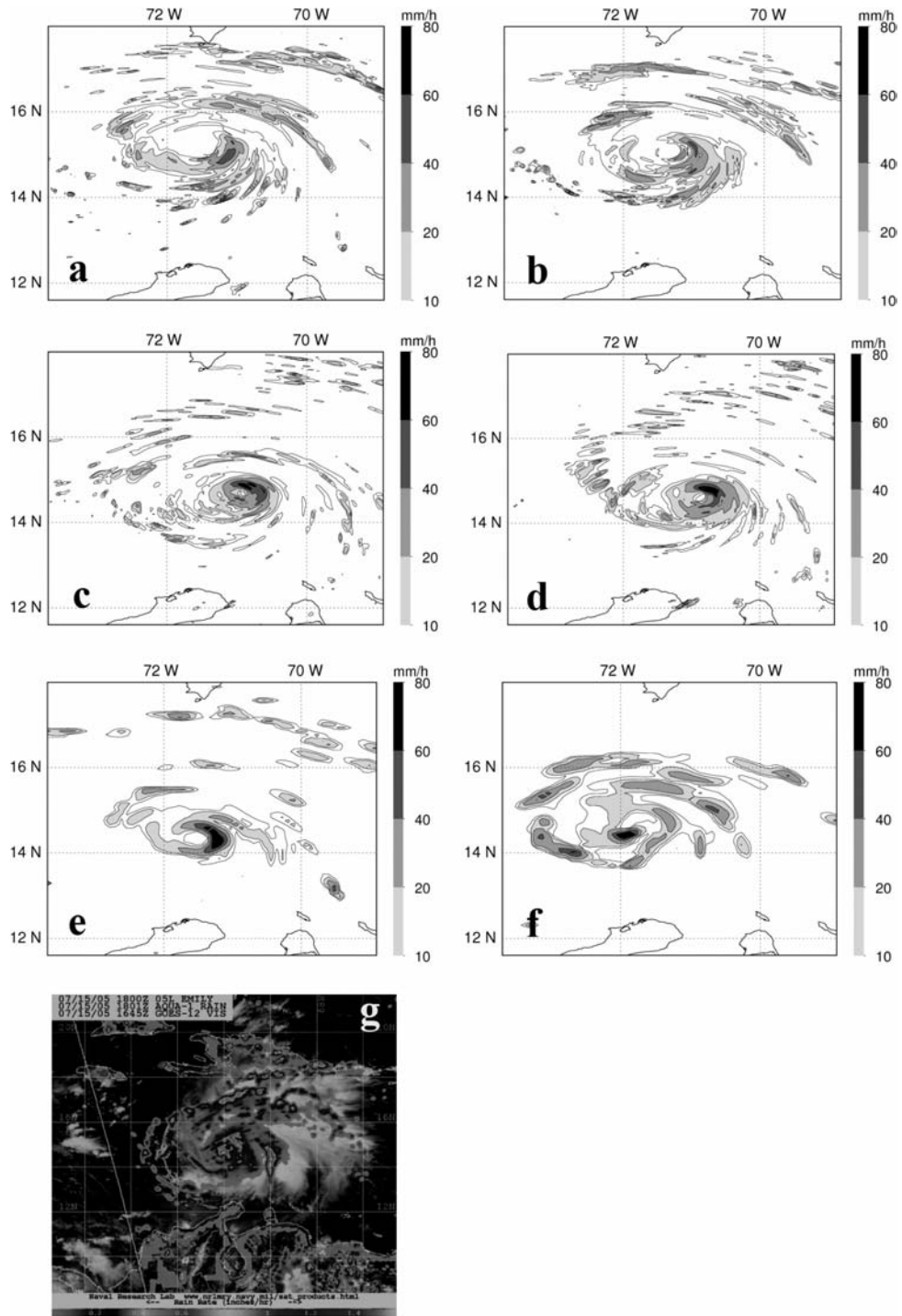
Fig. 11.   Hourly rainfall rate (mm/h) at 1800 UTC 15 July from different experiments, a) YSU3, b) YSUCU3, c) MYJ3, d) MYJCU3, e) YSUNOCU9, f) MYJNOCU9, compared with g) the rainfall rate (in/h) derived from Aqua AMSRE sensor at 1801 UTC 15 July 2005 (Courtesy of Naval Research Laboratory, Monterey, CA).
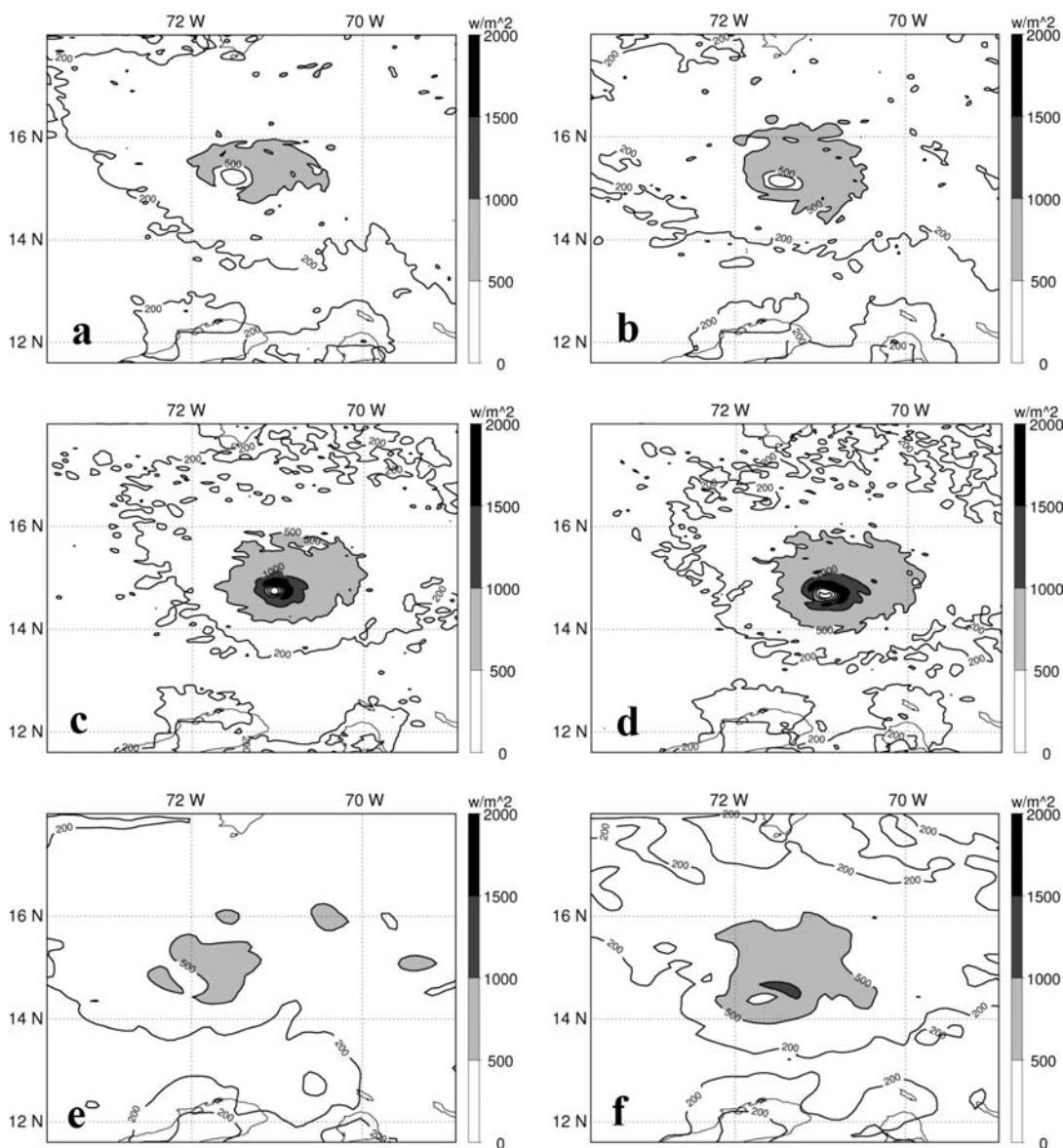
Fig. 12. Surface latent heat flux at 1800 UTC 15 July. a) YSU3, b) YSUCU3, c) MYJ3, d) MYJCU3, e) YSUNOCU9, and f) MYJNOCU9.

ence in the convective heating over the eyewall region is related to the strength of the convergent inflow in the lower troposphere and the divergent outflow in the upper troposphere.

3) The cumulus scheme is very important for the numerical simulation at 9 km resolution. Without the cumulus schemes, the model produces weak storm intensity due to weak and less organized vertical velocity in the eyewall and smaller surface latent heat flux in the storm inner core. In contrast, the use of the cumulus scheme at the 3 km grid spacing only causes a slight impact on storm intensity and structure.

4) At the 3 km grid spacing, PBL processes show a significant impact on the storm convective and precipitation structures and corresponding storm intensity. Up to a 37 hPa difference in minimum central SLP has resulted from the 54 h forecasts by
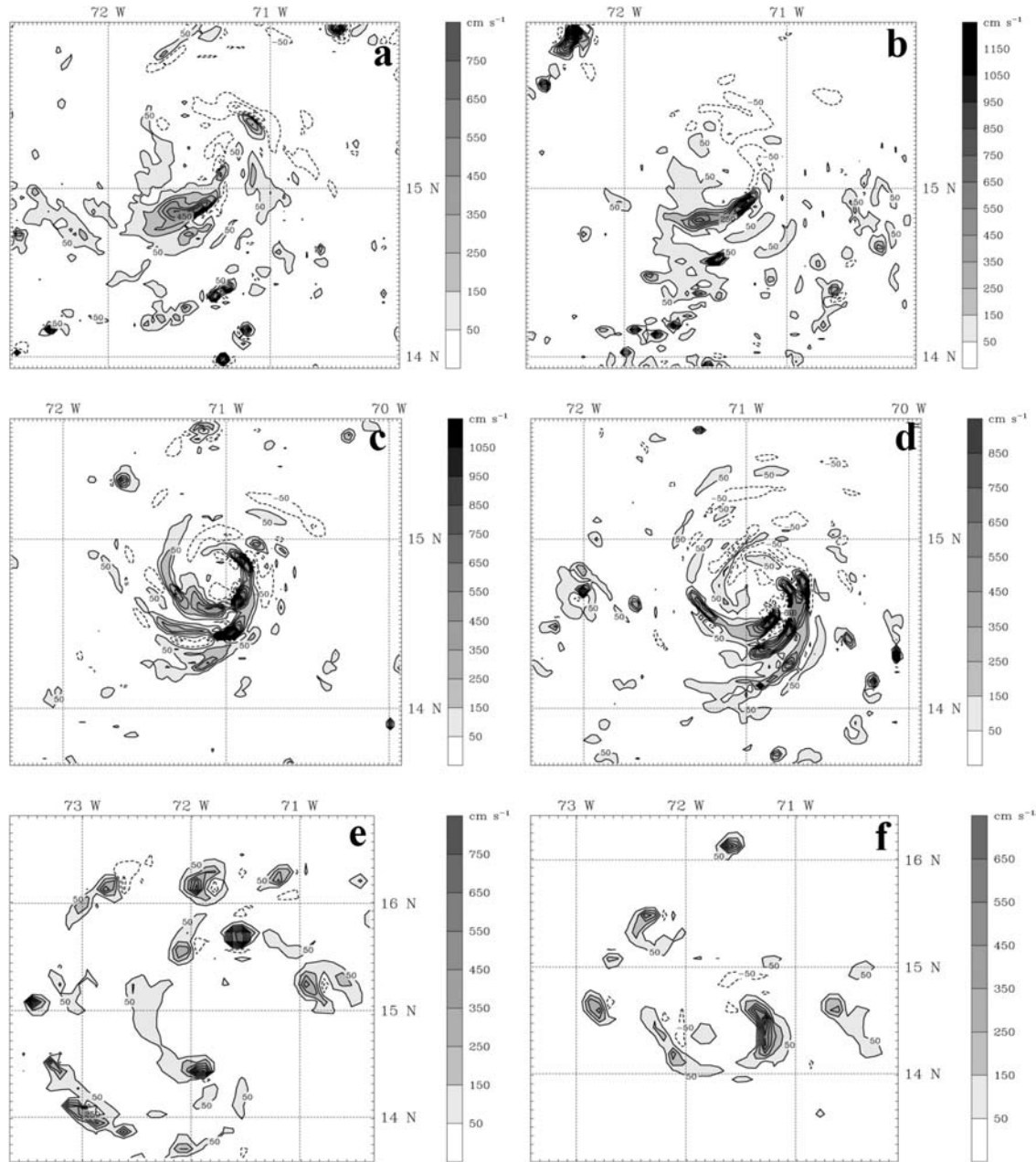
Fig. 13.   Vertical velocity at 500 hPa pressure level on 1800 UTC 15 July 2005 from experiments: a) YSU3, b) YSUCU3, c) MYJ3, d) MYJCU3, e) YSUNOCU9, and f) MYJNOCU9.

using different PBL schemes in the ARW model. In general, the MYJ PBL scheme causes deeper intensity of Emily than the YSU scheme does.

Although the results from this study shown strong sensitivity of hurricane intensity forecast to cumulus and PBL schemes, accurate intensity forecast of hurricane could also rely on many other physical processes and model resolution. Despite the results above, numerical simulation of Hurricane Emily's rapid intensification is also very sensitive to the choice of the microphysics schemes in WRF model (see detailed results in Li and Pu 2008). The signifi-

cant sensitivity of numerical simulations of Emily's rapid intensification to various model physical options indicates the great importance of physical processes and the complications of the use of physical parameterization schemes in producing accurate numerical forecasts of hurricanes' intensity change. More investigations are needed to further understand the physical and dynamic processes related to rapid hurricane intensification.

Acknowledgments

References

Betts, A. K., 1982: Saturation point analysis of moist convective overturning. *J. Atmos. Sci.*, **39**, 1484–1505.

Betts, A. K., and M. J. Miller, 1986: A new convective adjustment scheme. Part 2: Single column tests using GATE wave, BOMEX, ATEX, and arctic airmass data sets. *Quart. J. Roy. Meteor. Soc.*, **112**, 693–709.

Braun, S. A., and W. -K. Tao, 2000: Sensitivity of high-resolution simulations of Hurricane Bob (1991) to planetary boundary layer parameterizations. *Mon. Wea. Rev.*, **128**, 3941–3961.

Braun, S. A., M. T. Montgomery, and Z. Pu, 2006: High-resolution simulation of Hurricane Bonnie (1998). Part I: The organization of eyewall vertical motion. *J. Atmos. Sci.*, **63**, 19–42.

Byers, H. R., 1944: *General Meteorology*. McGraw-Hill, 645 pp.

Challa, M., and R. L. Pfeffer, 1984: The effect of cumulus momentum mixing on the development of a symmetric model hurricane. *J. Atmos. Sci.*, **41**, 1312–1319.

Davis, C. A., and K. A. Emanuel, 1988: Observational evidence for the influence of surface heat fluxes on rapid maritime cyclogenesis. *Mon. Wea. Rev.*, **116**, 2649–2659.

Davis, C. A., and L. F. Bosart, 2002: Numerical simulations of the genesis of Hurricane Diana. Part II: Sensitivity of track and intensity prediction. *Mon. Wea. Rev.*, **130**, 1100–1124.

Dudhia, J., 1989: Numerical study of convection observed during the winter monsoon experiment using a mesoscale two-dimensional model. *J. Atmos. Sci.*, **46**, 3077–3107.

Emanuel, K. A., 1995: Sensitivity of tropical cyclones to surface exchange coefficients and a revised steady-state model incorporating eye dynamics. *J. Atmos. Sci.*, **52**, 3969–3976.

Emanuel, K. A., 1999: Thermodynamic control of hurricane intensity. *Nature*, **401**, 665–669.

Franklin, J. L., and D. P. Brown, cited 2006: Tropical cyclone report: Hurricane Emily, 11–21 July 2005. National Hurricane Center Report. [Available online at http://www.nhc.noaa.gov/pdf/TCR-AL052005_Emily.pdf]

Grell, G. A., and D. Devenyi, 2002: A generalized approach to parameterizing convection combining ensemble and data assimilation techniques. *Geophys. Res. Lett.* **29**, Article 1693.

Hong, S. -Y., Y. Noh, and J. Dudhia, 2006: A new vertical diffusion package with an explicit treatment of entrainment processes. *Mon. Wea. Rev.*, **134**, 2318–2341.

Janjic, Z. I., 1994: The step-mountain eta coordinate model: further developments of the convection, viscous sublayer and turbulence closure schemes. *Mon. Wea. Rev.*, **122**, 927–945.

Janjic, Z. I., 2000: Comments on "Development and Evaluation of a Convection Scheme for Use in Climate Models", *J. Atmos. Sci.*, **57**, 3686.

Janjic, Z. I., 2002: Nonsigular Implementation of the Mellor-Yamada Level 2.5 Scheme in the NCEP global model. *NCEP Office Note*, **437**, 61pp. [Available at NCEP/EMC, 5200 Auth Road, Camp Springs, MD 20746].

Kain, J. S., and J. M. Fritsch, 1990: A one-dimensional entraining/detraining plume model and its application in convective parameterization. *J. Atmos. Sci.*, **47**, 2784–2802.

Kain, J. S., and J. M. Fritsch, 1993: Convective parameterization for mesoscale models: The Kain-Fritsch scheme. *The Representation of Cumulus Convection in Numerical Models, Meteor*. Monogr., **46**, Amer. Meteor. Soc., 165–170.

Kaplan, J., and M. DeMaria, 2003: Large-scale characteristics of rapidly intensifying tropical cyclones in the North Atlantic basin. *Wea. Forecasting*, **18**, 1093–1108.

Karyampudi, V. M., G. S. Lai, and J. Manobianco, 1998: Impact of initial conditions, rainfall assimilation, and cumulus parameterization on simulations of Hurricane Florence (1988). *Mon. Wea. Rev.*, **126**, 3077–33101.

Li, X., and Z. Pu, 2008: Sensitivity of numerical simulation of early rapid intensification of Hurricane Emily (2005) to cloud microphysical and planetary

boundary layer parameterizations. *Mon. Wea. Rev.*, **136**, 4819–4838.

Lin, Y. -L., R. D. Farley, and H. D. Orville, 1983: Bulk parameterization of the snow field in a cloud model. *J. Climate Appl. Meteor.*, **22**, 1065–1092.

Liu, Y., D. -L. Zhang, and M. K. Yau, 1997: A multi-scale numerical study of Hurricane Andrew (1992). Part I: explicit simulation and verification. *Mon. Wea. Rev.*, **125**, 3073–3093.

Malkus, J. S., and H. Riehl, 1960: On the dynamics and energy transformations in steady-state hurricanes. *Tellus*, **12**, 1–20.

McFarquhar, G. M., H. Zhang, G. Heymsfield, R. Hood, J. Dudhia, J. B. Halverson, and F. Marks Jr., 2006: Factors affecting the evolution of Hurricane Erin (2001) and the distributions of hydrometeors: role of microphysical processes. *J. Atmos. Sci.*, **63**, 127–150.

Mlawer, E. J., S. J. Taubman, P. D. Brown, M. J. Iacono, and S. A. Clough, 1997: Radiative transfer for inhomogeneous atmosphere: RRTM, a validated correlated-k model for the long-wave. *J. Geophys. Res.*, **102**, 16663–16682.

Rogers, R., S. Aberson, M. Black, P. Black, J. Cione, P. Dodge, J. Dunion, J. Gamache, J. Kaplan, M. Powell, N. Shay, N. Surgi, and E. Uhlhorn, 2006: The Intensity Forecasting Experiment: A NOAA multiyear field program for improving tropical cyclone intensity forecasts. *Bull. Amer. Meteor. Soc.*, **86**, 1523–1537.

Skamarock, W. C., J. B. Klemp, J. Dudhia, D. O. Gill, D. M. Barker, W. Wang, and J. G. Powers, 2005: *A description of the Advanced Research WRF Version 2* [available at Mesoscale and Microscale Meteorology Division, National Center for Atmospheric Research. Boulder, Colorado 80307].

Walsh, K., and I. G. Watterson, 1997: Tropical cyclone-like vortices in a limited area model: comparison with observed climatology. *J. Climate*, **10**, 2240–2259.

Willoughby, H. E., 1988: The dynamics of the tropical cyclone core. *Aus. Meteor. Mag.*, **36**, 183–191.

Zhu, T., and D. -L. Zhang, 2006: Numerical simulation of Hurricane Bonnie (1998). Part II: sensitivity to varying cloud microphysical processes. *J. Atmos. Sci.*, **63**, 109–126.